View metadata, citation and similar papers at core.ac.uk

brought to you by CORE

provided by Central Archive at the University of Reading

Investigations on the micellization of amphiphilic dendritic copolymers: from unimers to micelles

Article

Accepted Version

Creative Commons: Attribution-Noncommercial-No Derivative Works 4.0

Zhang, C., Zhou, H., Li, Y., Zhang, Y., Yu, C., Li, H., Chen, Y., Hamley, I. W. and Jiang, S. (2018) Investigations on the micellization of amphiphilic dendritic copolymers: from unimers to micelles. Journal of Colloid and Interface Science, 514. pp. 609-614. ISSN 0021-9797 doi: https://doi.org/10.1016/j.jcis.2017.12.070 Available at http://centaur.reading.ac.uk/75892/

It is advisable to refer to the publisher's version if you intend to cite from the work. See Guidance on citing.

Published version at: http://dx.doi.org/10.1016/j.jcis.2017.12.070

To link to this article DOI: http://dx.doi.org/10.1016/j.jcis.2017.12.070

Publisher: Elsevier

All outputs in CentAUR are protected by Intellectual Property Rights law, including copyright law. Copyright and IPR is retained by the creators or other copyright holders. Terms and conditions for use of this material are defined in the End User Agreement.

www.reading.ac.uk/centaur

University of Reading

CentAUR

Central Archive at the University of Reading

Reading's research outputs online

Investigations on the micellization of amphiphilic dendritic copolymers: from unimers to micelles

Cuiyun Zhang,[a,b,c] Huipeng Zhou,[a] Yongxin Li,[a] Yunyi Zhang,[a,b] Cong Yu,*[a,g] Hongfei Li,*[d,g] Yu Chen,*[e] Ian W. Hamley,*[f] Shichun Jiang*[b]

a. State Key Laboratory of Electroanalytical Chemistry, Changchun Institute of Applied Chemistry, Chinese Academy of Sciences, Changchun 130022, P. R. China.

b. School of Materials Science and Engineering, Tianjin University, Tianjin 300072, P. R. China.

c. Department of Chemistry, Key Laboratory of Advanced Textile Materials and Manufacturing Technology of the Education Ministry, Zhejiang Sci-Tech University, Hangzhou 310018, China.

d. State Key Laboratory of Polymer Physics and Chemistry, Changchun Institute of Applied Chemistry, Chinese Academy of Sciences, Changchun 130022, P. R. China.

e. Department of Chemistry, School of Sciences, Tianjin University, Tianjin 300072, P. R. China.

f. School of Chemistry, Pharmacy and Food Biosciences, University of Reading, Whiteknights, Reading RG6 6AD, United Kingdom.

g. University of Chinese Academy of Science, Beijing, 100049, P. R. China.

Corresponding author and Email:

Cong Yu, congyu@ciac.ac.cn;

Hongfei Li, hfli@ciac.ac.cn;

Yu Chen, chenyu@tju.edu.cn;

Ian W. Hamley, i.w.hamley@reading.ac.uk;

Shichun Jiang, scjiang@tju.edu.cn.

Abstract:

Since the micellization kinetics is influenced by polymer structure, the spherical three-dimensional topology of amphiphilic dendritic copolymers (ADPs) which hinders the phase separation during micellization is assumed to make the micellization kinetics different. In the literatures, most of the attention has been paid to the morphology transition or the morphology at equilibrium and the micellization kinetics of ADPs is rarely reported. In this study, the micellization processes of amphiphilic dendritic copolymers from unimers to the final equilibrium micelles were monitored by laser light scattering. Based on the closed association mechanism, the thermodynamics of micellization was analysed. The negative thermodynamic quantities indicate that the micellization of ADPs is driven by enthalpy. Based on the change of scattering intensity and hydrodynamic radius (R_h) with time, the detailed micellization kinetics was analysed, which contains two steps. By controlling the temperature and type of solvent, a system in which the concentration has little influence on R_h is obtained. The relaxation times of the two steps decrease with concentration, indicating that at higher concentration the rate of micellization is quicker. With the increasing mass fraction of the hydrophobic part, the relaxation times decrease and the driving force of micellization increases.

Key words: Amphiphilic dendritic copolymers; Micellization; Kinetics; Concentration; Relaxation times

1. Introduction

Micellization of surfactants and block copolymers has been investigated extensively [1-4]. However, the theoretical investigations on the micellization kinetics of amphiphilic dendritic copolymer have been greatly lagged behind the surfactants and linear polymer. The micellization processes can be investigated using time-resolved small-angle X-ray scattering, stopped-flow light scattering, etc. [5,6]. Usually, micellization is caused by the abrupt change of the solvent quality, pH or temperature.

Temperature is an important factor in controlling the physical and chemical processes of a polymer solution. Above or below a critical temperature, thermosensitive polymers undergo a phase transition from a soluble to an insoluble state. The aqueous solution of a poly(N-isopropylacrylamide) polymer usually exhibits a lower critical solution temperature (LCST) behaviour [7], while polymers such as polystyrene-poly(tert-butylstyrene) in a nonsolvent exhibit a upper critical solution temperature (UCST) [8,9]. Three temperature regions corresponding to the state of stable unimers, the unimer-micelle transition and the micellar state were found with the change of temperature in the micellization processes [8]. The thermodynamics of different micellizing systems have been investigated [9]. Usually, the micellization of a polymer in an organic solvent with a UCST is driven by the enthalpy and the entropy-driven processes are favoured for aqueous polymer solutions with a LCST.

For surfactants, the Aniansson and Wall theory has been widely accepted to

descrip the micellization processes, in which only the insertion/expulsion of individual unimers is included [1]. In the first step of micellization, the aggregation number of the micelles redistributes, while the micelle number remains constant. In the following step, through formation and decomposition processes, the micelle number changes and the micellization process approaches equilibrium. Honda et al. reported the micellization of block copolymers [3]. The unimers quickly associated to form quasi-equilibrium micelles and the number of micelles increased in the first step. Accompanying the deformation of the quasi-equilibrium micelles, the micelle size grows and the micellization in the second step finally approaches equilibrium. Compared with surfactants and block copolymers, the compact structure of the amphiphilic dendritic copolymers hinders the phase separation during themicellization process [10], which makes the micellization behaviors different.

Compared to surfactants and amphiphilic block copolymers, amphiphilic dendritic copolymers are new members in the family of amphiphilic molecules. The self-assembly behaviors of amphiphilic dendritic copolymers have been actively investigated in the past decades [11-15]. Various morphologies such as micelles, vesicles, filers have been reported [16-18] and micelles are the most prevalent structure. The fusion and fission process of vesicles which are large enough for observation by the optical microscopy has been observed in detail [19.20]. The multimicelle aggregation mechanism (MMA) was reported by Yan et al. and they proposed that the large micelles are the secondary aggregation of the unimers [11,12]. The detailed aggregation processes of the amphiphilic dendritic copolymers were

explored with dissipative particle dynamics simulation [21]. In this simulation, by varying the interaction parameters of the hydrophobic core, hydrophilic shell and water (solvent), different micellization mechanisms are observed, which are the unimolecular micelle aggregation mechanism and the small micelle aggregation mechanism. The former is the direct aggregation of the unimers, whereas in the small micelle aggregation mechanism, the large micelles are the secondary aggregation of the microphase-separated small micelles. Except for the computer simulation, little attention has been paid to the micellization kinetics of the amphiphilic dendritic copolymers.

In our previous reports [22], we have investigated the micellization processes of the ADPs by mixing of a selective solvent with a common solvent, in which two steps could be distinguished clearly and this is the first time the detailed micellization kinetics has been studied. In the first step the small micelles quickly associate to form larger micelles and in the second step accompanying the fission and fusion of micelles, the aggregation approaches dynamical equilibrium. However, due to the solvent mixing, filtration in the sample preparation and the quick association of the unimers, the initial formation information of the micelles is missing and the analysis of micellization is mainly focused on the fusion of small micelles. In this work, in order to track the aggregation processes from unimers to the final equilibrium micelles of the ADPs, after filtration the temperature was controlled to a critical value at which all the ADPs can undergo micellization. Also, in the previous reports [22], the influence of concentration on the relaxation times is contrary to the block copolymers and by

analysing the micelle concentration, we found that the increasing relaxation time is caused by the decreasing micelle concentration with increasing unimer concentration. For a comprehensive understanding of the relation of micelle size and relaxation time of the ADPs, in this study, we choose a system in which the unimer concentration has little influence on the micelle size. The change of relaxation times is caused only by the unimer concentration and DA.

In this paper, first, the critical micellization temperature (cmt) at which micellization starts was measured. Second, the thermodynamics of micellization was studied. Then the influence of the concentration and DA on the micellization processes were investigated and discussed. Based on the temperature-jump methods, the micellization processes of the ADPs from unimers to the final equilibrium micelles were explored.

2. Materials and methods

2.1. Materials

The ADPs were synthesized according to the literature [23] and the synthesis steps are shown in **Scheme S1**. DA is the percentage of the amino groups in hyperbranched polyethyleneimine which react with the dendritic palmitate chains. The structural parameters are listed in **Table S1**.

2.2 Methods

The time-dependent scattering intensity and hydrodynamic radius were measured by an ALV CGS-3 light scattering spectrometer. The average radius of gyration (R_g) of the micelles was calculated according to the Guinier plot $\ln(I_q) = \ln(I_0) - q^2R_g^2/3$,

where I_q is the intensity at the scattering vector q and I_0 is the intensity in the q=0 limit. The restriction of the Guinier plot is $qR_g<1$ [24]. The scattering vector $q = (4\pi n/\lambda)\sin(\theta/2)$, n is the refractive index of the solvent, λ is the wavelength of the light, θ is the scattering angle. From Laplace inversion of the intensity-intensity time correlation function, the distribution function of the decay rate can be obtained and the average decay rate (Γ) at different angles can be calculated. From the equation $\Gamma = Dq^2$, the diffusion coefficient (D) can be obtained. Based on the Stokes-Einstein equation $R_h = k_BT/6\pi\eta D$, the average hydrodynamic radius was calculated, where k_B is the Boltzmann constant, T is the absolute temperature and η is the solvent viscosity [25,26]. The temperature was controlled by a circulator bath and the accuracy is 0.02 °C. The solutions of ADPs in the laser light scattering were filtered with millipore filters (0.22 μm).

3. Results and discussions

3.1 The critical micellization temperature of the ADPs

Because of the strong dependence of the scattering intensity on the volume of the scatterer, light scattering is a powerful tool to detect the onset of micellization. By increasing concentration or changing temperature, the micellization of a polymer solution can be initiated. For the ADPs with a hydrophilic core and a hydrophobic shell, glycol dimethyl ether with a low polarity is a poor solvent [10]. The ADPs in glycol dimethyl ether undergo micelle formation with the decrease of temperature, which leads to an increase of scattering intensity. The change of scattering intensity with temperature is shown in **Fig. 1** and the scattering intensity increase sharply in a

narrow temperature range with decreasing temperature. The corresponding temperature of the transition point in **Fig. 1** is the cmt. The polarity of the ADPs decreases with increasing DA which induces a poor solubility of the ADPs at higher DA and, at a given concentration, the cmt increases with increasing DA (**Fig. S1**).

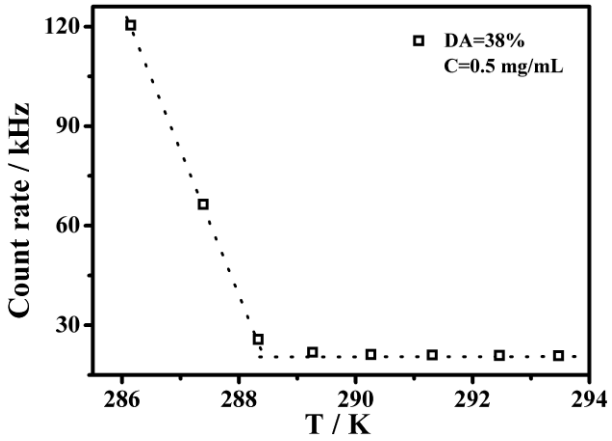

Fig. 1. The change of scattering intensity with temperature for P-1 at 0.5 mg/mL.

3.2 Thermodynamics of ADPs micellization

A thermodynamic analysis is essential to understand the micellization processes. The experiment methods to obtain the thermodynamic parameters mainly contain two approaches [9]. The first is the direct measurement of the enthalpy by differential scanning calorimetry. In this experiment, Because of the low mass percent (<0.05%), the errors arising from the evaporation of solvent and other aspects cannot be ignored and this method is invalid. The second is based on the closed association model to estimate the thermodynamic parameters. The micellization system with a large aggregation number and narrow micelle size distribution obeys the closed association model [8,9,27]. The standard free energy (ΔG_0) and standard enthalpy (ΔH_0) of micelle

formation can be estimated by eq1 and eq 2, where R = 8.314 J/(mol K) and cmc is the critical micelle concentration at the temperature T.

$$\Delta G^0 = RT \ln(cmc) \quad (1)$$

$$\Delta H^0 = R\left[d \ln(cmc) / d(1/T)\right] \quad (2)$$

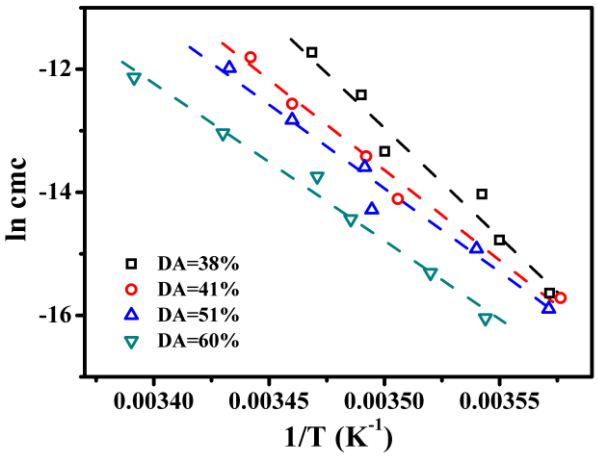

Fig. 2. Logarithmic of critical micelle concentration as a function of the reciprocal of temperature.

Table 1 The thermodynamic quantities of the ADPs.

DA	38%	41%	51%	60%
ΔH^0/kJ mol^{-1}	-290	-241	-234	-213
ΔG^0/ kJ mol^{-1}	-36	-37	-37	-38
$T\Delta S^0$/kJ mol^{-1}	-254	-205	-197	-176

Here, the cmc and T can be replaced by the concentration and cmt. By the integration of eq 2, eq 3 is obtained and a is an arbitrary constant. Through the linear fitting of ln(cmc) versus 1/T, the values of ΔH_0 can be calculated (**Fig.**

2). The correlation coefficients of the linear fitting in **Fig. 2** are above 0.95. The values of ΔG_0 and standard entropy (ΔS_0) were calculated according to eq 1 and eq 4 at C = 0.01 mg/mL. The thermodynamic quantities are shown in **Table 1**. The negative thermodynamic quantities indicate that the micellization is driven by enthalpy and the formation of micelles is an exothermic process. The negative enthalpy results from the attractive interaction from the insoluble part of the ADPs. On the contrary, the entropic factors tend to disperse the ADPs randomly in solution. The influence of enthalpy outweighs the entropy, which leads to the micellization of ADPs.

$$\ln(cmc) = \frac{\Delta H_0}{RT} + a \quad (3)$$

$$\Delta S_0 = (\Delta H_0 - \Delta G_0) / T \quad (4)$$

3.3 The micellization kinetics of the ADPs

The time scale of the micellization of block copolymers ranges from milliseconds to hours depending on the micellization conditions [3,10,28-31]. For poly(ethylene-alt-propylene)-poly (ethylene oxide), the micellization is completed within hundreds of seconds [31]. The micellization was considered as a nucleation and growth type governed by the unimer insertion or expulsion mechanism, in which the micelle size and overall rate increase with concentration. The micellization of poly(α-methylstyrene)-block-poly (vinylphenethyl alcohol) in selective solvent takes tens of hours with a fast step and slow step, and the weight of the micelle increase with concentration [3].

For triblock copolymers, the micellization processes involves both the fusion of small micelles (the first step) and the insertion/expulsion of copolymer chains (the second step) [32]. The relaxation time decreases with increasing concentration and the diffusion coefficient of the unimers is constant, which leads to decreasing micelle size of the triblock copolymers with increasing concentration [32]. Dissipative particle dynamics simulation results show that the aggregation number of the micelles keeps constant with the increasing concentration [33]. For amphiphilic hyperbranched copolymers, the micelle size increases with increasing concentration [34]. The micellization kinetics and micelle size are related to the particular polymer in the amphiphiles and the micellization conditions. Both the relaxation times and the micelle size are strongly dependent on the polymer, solvent, temperature, etc.

The experimental temperature was set to be 276.15 *K*, which is lower than the cmt. At the temperatures higher than 276.15 *K*, the distribution of the micelles is polydisperse and the phenomenon is unfavorable for the analysis of the kinetics. As shown in **Fig. 3**, the scattering intensity increases from the values corresponding to the unimers to larger values corresponding to the final equilibrium micelles with a rapid increase followed by a slow increase, which are the first step and the second step. The time-dependent scattering intensity of P-2, P-3 and P-4 was shown in **Fig. S2**. The results in **Fig. 4** are the change of R_h with time and the increasing trend is the same as for the scattering intensity (**Fig. S3**).

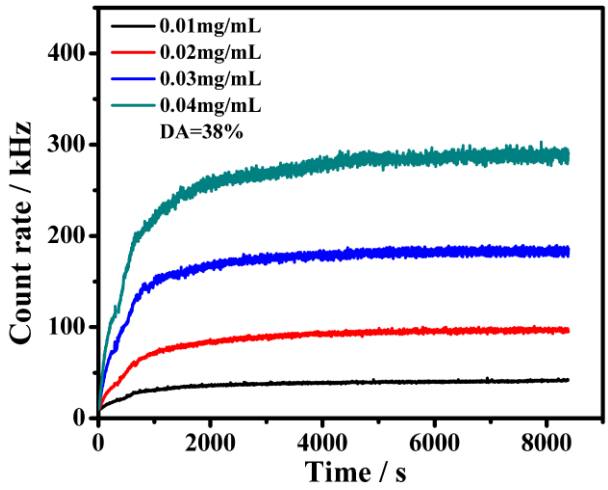

Fig. 3. Time-dependent scattering intensity of P-1 at different concentration.

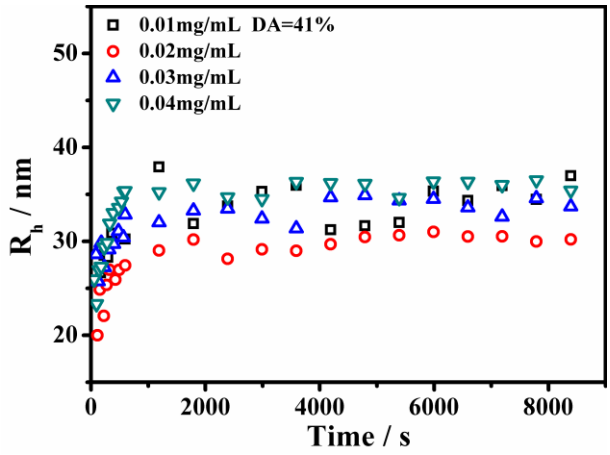

Fig. 4. Time-dependent hydrodynamic radius of P-2 at different concentrations.

The R_h of the micelles increases with the unimer concentration in the solvent mixture of chloroform and methanol as previously reported [22]. However, in the present system, the influence of the unimer concentration on the micelle size is different. The values of R_h change little with increasing concentration (**Fig. 4** and **Fig. S4**). It is known that the scattering intensity of the solution is related to the micelle size and the number density of the micelles. As shown in **Fig. 4**, the scattering intensity increases with the concentration. The weak change of R_h with concentration indicates that the increasing scattering intensity arises from the increasing number density of the micelles. **Fig. S5a** shows the change of decay rate and scattering

intensity with scattering vector. The values of R_h and R_g of the micelles were calculated according to the Stokes-Einstein equation and the Guinier plot respectively. In **Fig. S5b**, the ratio of R_g and R_h is around 0.775, indicating that the morphology of aggregates at equilibrium is micelle [35-37]. The values of the R_g of the four ADPs at 0.04 mg/L are 38 nm, 28 nm, 25 nm, and 17 nm, which is consistent with the micelle size obtained from transmission electron microscope (TEM) images (**Fig. S6**).

In order to prove that during the micellization processes the morphology of the aggregates is spherical micelles, the aggregates were observed by TEM at 300 s and 600 s after the micllization began. As shown in Fig. S7, the average size of the spherical micelles is 12 nm (300 s) and 16 nm (600 s). Also, the ratio of R_g and R_h after 2000s was calculated and the values are around 0.775 (Fig. S8). These results indicate that the morphology of the aggregates is spherical micelles during the whole micellization processes.

The relaxation processes of the micellization of ADPs were analyzed according to the surfactants and block copolymers [1,5]. The function of the normalized scattering intensity and time can be fitted by using a double exponential function (eq 5). Where I_∞ is the scattering intensity at infinitely long time, C_1 and C_2 are the normalized amplitudes ($C_1 + C_2 = 1$), τ_1 and τ_2 are the relaxation times of the two steps. The mean micelle formation constant, τ_f , can be calculated according to eq 6.

$$(I_\infty - I_t)/I_\infty = C_1 e^{-t/\tau_1} + C_2 e^{-t/\tau_2} \quad (5)$$

$$\tau_f = C_1\tau_1 + C_2\tau_2 \quad (6)$$

Because of the rapid aggregation of the unimers and fusion of the small micelles,

the scattering intensity changes suddenly at early stage of the first step. The value of R_h which is obtained from the CONTIN Laplace inversion of the intensity-intensity time correlation function cannot be calculated at the early stage in the first step. However, the change of scattering intensity maps that of R_h (**Fig. S3**), so the kinetic processes of the micellization are expressed by the evolution of scattering intensity. As shown in **Fig. S9** and **Fig. 5**, the relaxation times τ_1, τ_2 and τ_f decrease with concentration, indicating that the aggregation approaches equilibrium quicker at higher concentration. In the previous report, the micelle size increases with concentration, which induces the lower micelle concentration at higher unimer concentration [22]. The concentration dependent fission and fusion of the micelle is based on the mechanism of collision. The lower micelle concentration at higher unimer concentration leads to an increase in relaxation time, which is different from the results in this system.

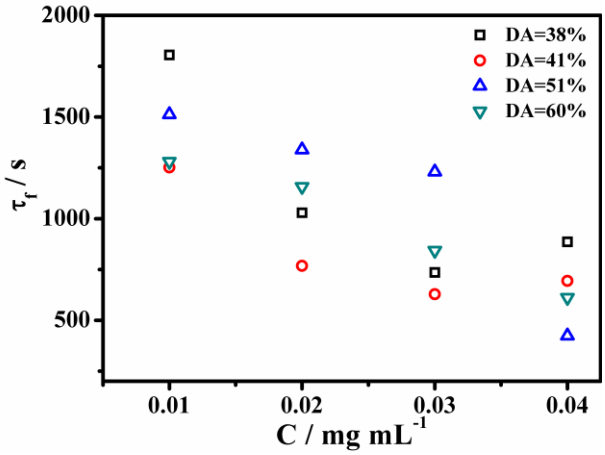

Fig. 5. Plot of τ_f vs concentration.

Unimer entry/expulsion and micelle fusion/fission are the two micellization mechanisms of block copolymers. For block copolymers, the unimer entry/expulsion

is faster than the fusion and fission of micelles at equilibrium [32]. In the second step, the concentration of the unimers is close to the critical micelle concentration [5,32].[5,32] The unimer entry/expulsion mechanism in the second step leads to the independence of the relaxation time on the unimer concentration, while, the relaxation time of the fusion/fission is inversely proportional to the concentration [38]. The decreasing τ_2 with concentration illustrates that the second step of the aggregation is consistent with the fusion/fission mechanism. Though the relaxation time in the previous and present report is different, the fission and fusion mechanism is the same and the time scale of the micellization is dependent on the solvent, polymer, temperature.

As micellization proceeds, the micelle size distribution of block copolymes becomes narrower [3]. The distribution functions of the micelle are shown in **Fig. 6** and **Fig. S10**. The black lines in **Fig. 6** are the distributions of R_h of the unimers at room temperature in glycol dimethyl ether. Compared with the distribution of the unimers at room temperature, shortly after the beginning of the aggregation, almost all of the unimers aggregate to form micelles. At lower concentration, the distribution of micelles in the initial stage is broader and gradually becomes narrower. The polydispersity index (PDI) of the distribution of the micelles is shown in **Fig. S11**, which is broader in the first step and narrower in the second step.

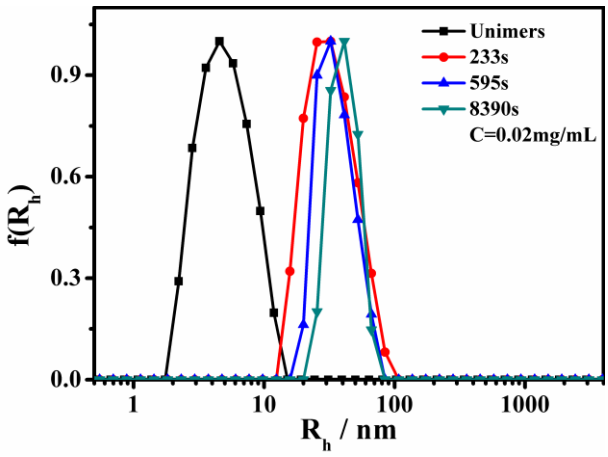

Fig. 6. Time-dependent distribution of R_h for P-1 at 0.02 mg/mL.

The micellization processes of the ADPs can be illustrated by **Scheme 1**. The sudden change of the scattering intensity is caused by the quick association of the uinmers to form small micelles and the fusion of small micelles to large micelles in the first process of the micellization. The fission and fusion occurs among the micelles in the second process, which cause the size and number of micelles to change with time. The micellization processes (**Scheme 1**) agree well with the MMA mechanism which is proposed by Yan et al. [11,12].

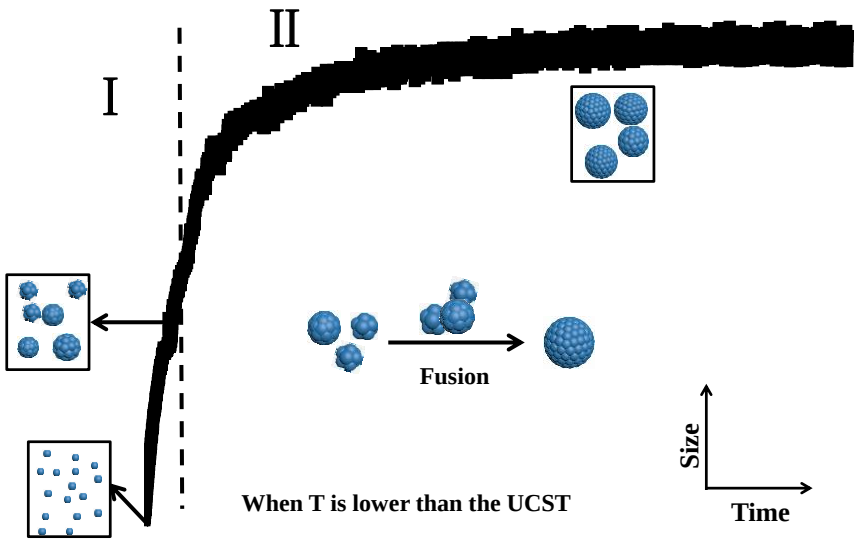

Scheme 1. The proposed micellization steps of the ADPs.

3.4 Influence of DA on the micellization kinetics

The driving force for the micellization of amphiphilic block copolymers increases with increasing chain length of the insoluble part and the micellization mechanism of the slow step transformed from the unimer insertion/expulsion to micelle fusion/fission [39]. The micelle size and aggregation number increase with increasing size of the insoluble part. For amphiphilic hyperbranched copolymers, the micelle size increases with increasing weight fraction of the insoluble part in water [15]. **Fig. 7** shows the dependence of the scattering intensity on DA at the same unimer molar concentration. For P-1, P-2 and P-3, the scattering intensity increases with DA, while for P-4 the scattering intensity in the first step is stronger than P-1 and in the second step the scattering intensity is almost the same with P-1. In order to understand this phenomenon, the values of the average hydrodynamic radius were

calculated. The R_h decreases with DA as shown in **Fig. 8**, which is contrary to the previous reports [22], and this will be explained later. For P-1, P-2 and P-3 the increasing scattering intensity results from the increasing number density of the micelles with DA.

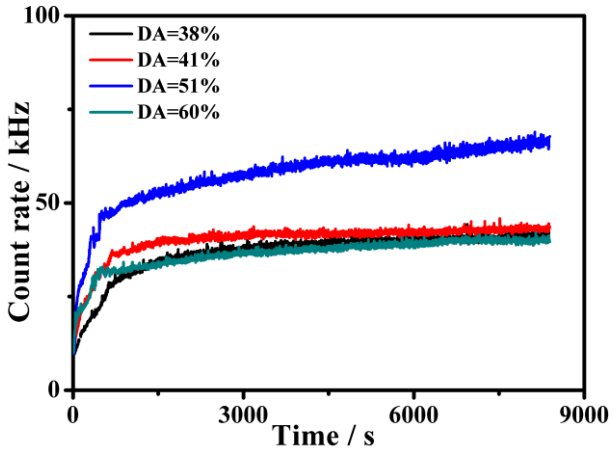

Fig. 7. Time-dependent scattering intensity of the ADPs with different DA.

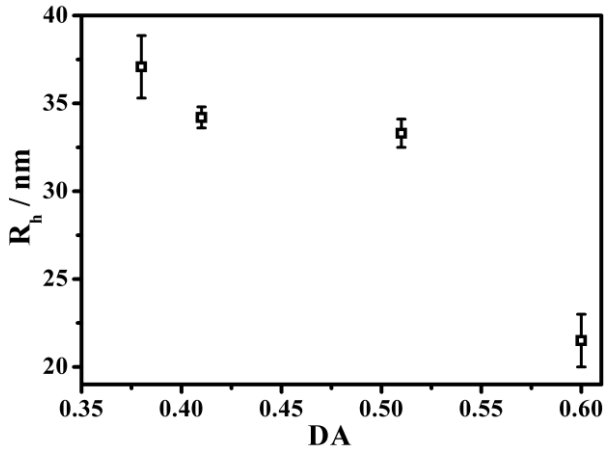

Fig. 8. Change of the R_h with DA.

Table 2. The relaxation time of the ADPs at 6×10^{-11} mol/mL.

DA	38%	41%	51%	60%
τ_1/s	602.5	372.5	241.6	204.0
τ_2/s	6556.8	4687.5	4872.7	4088.7
τ_f/s	1805.3	1781.6	1777.5	1267.3

It is known that the nonpolarity of the ADPs increases with DA. Although glycol dimethyl ether is a weak polar solvent, the solubility of the ADPs decreases as DA increases. **Table 2** shows that τ_1, τ_2 and τ_f decrease with DA, indicating that with increasing DA, the driving force for the aggregation increases. For the ADPs in the solvent mixture [22], because of the decreasing micelle concentration, the relaxation times (τ_1, τ_2) increase with the unimer concentration, which is different from the phenomenon in this system. The diffusion coefficients of the ADPs unimers at 6×10^{-11} mol/mL decrease with DA (Table S1). The smaller τ_f means that the micelles take shorter time to grow. The decreasing diffusion coefficient of the unimers and smaller τ_f indicate that at higher DA less unimers will be incorporated into the micelles and the micelle size is smaller [32]. The scattering intensity is proportional to the sixth power of the micelle size. For P-4, the increasing number density of micelles cannot make up the losing scattering intensity caused by the micelle size, so the scattering intensity of P-4 is weaker (**Fig. 7**).

Conclusions

The temperature induced micellization of the ADPs was investigated by laser light scattering. When the temperature jumps from room temperature to the cmt, the micellization of the ADPs begins due to the decreasing solubility and this behavior is induced by the enthalpic factors. According to the change of scattering intensity and R_h with time, the micellization was divided into two steps with different relaxation times. The quick association of the unimers and fusion of the small micelles lead to the rapid increase of the micelle size in the first step. In the second step, through the

fission and fusion of the micelle, the micelle size increases gradually and finally approaches equilibrium. Changing concentration has little effect on R_h. The decrease in relaxation time with concentration means a quicker aggregation rate. At higher DA, the content of nonpolar part increases, so the solubility of the ADPs decreases, which means that the driving force of micellization is stronger at higher DA. Because of the decrease in unimers diffusion coefficient and relaxation time with DA, the R_h of the micelles decreases. These results are not in conflict with our previous report (Zhang et al. Macromolecules, 2017, 50, 1657). The different influence of the concentration and DA on the micellization kinetics is due to the use of a different solvent and the change of temperature as a driver of micellization. On the other hand, this phenomenon illustrates that the micellization kinetics is complicated and dependent on the polymer, solvent and temperature. The in situ study of the micellization kinetics is consistent with the previous assumption, which illustrates the micellization in a MMA mechanism [11, 12]. Except for the optical microscopy for the observation of the fusion and fission of larger aggregates [19, 20], laser light scattering is an effective method to study the kinetics of smaller aggregates. The understanding of micellization kinetics is beneficial to optimize the application of the micelles in the field of drug delivery, biosensing etc. [40-42]. In the future study, the influence of the degree of branching of the core on the aggregation kinetics will be studied.

Acknowledgements

This work was supported by the National Nature Science Foundation of China

(21374077, 51573131, 21561162004 and 21405151), the Science and Technology Development Project (International Collaboration Program) of Jilin Province (20160414040GH) and Science Foundation of Zhejiang Sci-Tech University (No. 17062155-Y). The Royal Society (UK) is thanked for an International Collaboration Grant (ref. IE140849).

Notes and references

[1] E. A. G. Aniansson and S. N. Wall, J. Phys. Chem., 78 (1974), 1024-1030.

[2] E. A. G. Aniansson, S. N. Wall, M. Almgren, H. Hoffmann, I. Kielmann, W. Ulbricht, R. Zana, J. Lang and C. Tondre, J. Phys. Chem., 80 (1976), 905-922.

[3] C. Honda, Y. Hasegawa, R. Hirunuma and T. Nose, Macromolecules, 27 (1994), 7660-7668.

[4] E. E. Dormidontova, Macromolecules, 32 (1999), 7630-7644.

[5] Y. Zhang, T. Wu and S. Liu, Macromol. Chem. Phys. 208 (2007), 2492-2501.

[6] G. V. Jensen, R. Lund, J. Gummel, M. Monkenbusch, T. Narayanan and J. S. Pedersen, J. Am. Chem. Soc., 135 (2013), 7214-7222.

[7] C. Chang, H. Wei, J. Feng, Z.-C. Wang, X.-J. Wu, D.-Q. Wu, S.-X. Cheng, X.-Z. Zhang and R.-X. Zhuo, Macromolecules, 42 (2009), 4838-4844.

[8] Z. Zhou, B. Chu and D. G. Peiffer, Macromolecules, 26 (1993) , 1876-1883.

[9] H. W. Shen, L. F. Zhang and A. Eisenberg, J. Phys. Chem. B, 101 (1997), 4697-4708.

[10] C. Zhang, C. Yu, Y. Lu, H. Li, Y. Chen, H. Huo, I. W. Hamley and S. Jiang, Polym. Chem., 7 (2016), 3126-3133.

[11] Y. Y. Mai, Y. F. Zhou and D. Y. Yan, Macromolecules, 38 (2005) , 8679-8686.

[12] H. Hong, Y. Mai, Y. Zhou, D. Yan and J. Cui, Macromol. Rapid Commun., 28 (2007) , 591-596.

[13] Y. Liu, C. Yu, H. Jin, B. Jiang, X. Zhu, Y. Zhou, Z. Lu and D. Yan, J. Am. Chem. Soc., 135 (2013) , 4765-4770.

[14] W. Jiang, Y. Zhou and D. Yan, Chem. Soc. Rev., 44 (2015) , 3874-3889.

[15] H. Cheng, X. Yuan, X. Sun, K. Li, Y. Zhou and D. Yan, Macromolecules, 43 (2010), 1143-1147.

[16] M. R. Radowski, A. Shukla, H. von Berlepsch, C. Böttcher, G. Pickaert, H. Rehage and R. Haag, Angew. Chem. Int. Ed., 46 (2007), 1265-1269.

[17] A.-M. Caminade, D. Yan and D. K. Smith, Chem. Soc. Rev., 44 (2015), 3870-3873.

[18] M. Ornatska, K. N. Bergman, M. Goodman, S. Peleshanko, V. V. Shevchenko and V. V. Tsukruk, Polymer, 47 (2006), 8137-8146.

[19] Y. F. Zhou and D. Y. Yan, J. Am. Chem. Soc., 127 (2005) , 10468-10469.

[20] Y. F. Zhou and D. Y. Yan, Angew. Chem. Int. Ed., 44 (2005), 3223-3226.

[21] Y. Wang, B. Li, Y. Zhou, Z. Lu and D. Yan, Soft Matter, 9 (2013), 3293-3304.

[22] C. Zhang, Y. Fan, Y. Zhang, C. Yu, H. Li, Y. Chen, I. W. Hamley, and S. Jiang, Macromolecules, 50 (2017), 1657-1665.

[23] Y. Liu, Y. Fan, X.-Y. Liu, S.-Z. Jiang, Y. Yuan, Y. Chen, F. Cheng, and S.-C. Jiang, Soft Matter, 8 (2012), 8361-8369.

[24] Gunier and G. Fournet, Small Angle Scattering of X-rays, 1955.

[25] C. Wu and K. Q. Xia, Rev. Sci. Instrum., 65 (1994), 587-590.

[26] B. Chu and F. L. Lin, J. Chem. Phys., 61 (1974), 5132-5146.

[27] W. Hamley, Introduction to Soft Matter, 2007.

[28] J. Rao, J. Zhang, J. Xu and S. Liu, J. Colloid Interface Sci., 328 (2008), 196-202.

[29] L. Chen, H. W. Shen and A. Eisenberg, J. Phys. Chem. B, 103 (1999), 9488-9497.

[30] S. E. Burke and A. Eisenberg, Langmuir, 17 (2001), 6705-6714.

[31] K. Iyama and T. Nose, Macromolecules, 31(1998), 7356-7364.

[32] Z. Y. Zhu, S. P. Armes and S. Y. Liu, Macromolecules, 38 (2005), 9803-9812.

[33] Z. Li and E. E. Dormidontova, Macromolecules, 43 (2010), 3521-3531.

[34] F. L. Hatton, P. Chambon, T. O. McDonald, A. Owen and S. P. Rannard, Chem. Sci., 5 (2014), 1844-1853.

[35] Y. F. Tu, X. H. Wan, D. Zhang, Q. F. Zhou and C. Wu, J. Am. Chem. Soc., 122 (2000) , 10201-10205.

[36] H. Huo, K. Li, Q. Wang and C. Wu, Macromolecules, 40 (2007), 6692-6698.

[37] I. W. Hamley, C. Daniel, W. Mingvanish, S.-M. Mai, C. Booth, L. Messe and A. J. Ryan, Langmuir, 16 (2000), 2508-2514.

[38] F. J. Esselink, E. Dormidontova and G. Hadziioannou, Macromolecules, 31 (1998), 2925-2932.

[39] J. Zhang, J. Xu and S. Liu, J. Phys. Chem. B, 112 (2008), 11284-11291.

[40] M. Prabaharan, J. J. Grailer, S. Pilla, D. A. Steeber, S. Gong, Biomaterials, 30

(2009) , 3009-3019.

[41] H. Shi, C. Xiujie, S. Liu, H. Xu, Z. An, L. Ouyang, Z. Tu, Q. Zhao, Fan, Q. Wang, L. Huang, W. ACS Appl. Mater. Interfaces, 5 (2013), 4562-4568.

[42] S. Yu, R. Dong, J. Chen, F. Chen, W. Jiang, Y. Zhou, X. Zhu, D. Yan, Biomacromolecules, 15 (2014), 1828-1836.

Figure Captions

Fig. 1. Scattering intensity vs temperature.

Fig. 1. The change of scattering intensity with temperature for P-1 at 0.5 mg/mL.

Fig. 2. Logarithmic of critical micelle concentration as a function of the reciprocal of temperature.

Fig. 3. Time-dependent scattering intensity of P-1 at different concentration.

Fig. 4. Time-dependent hydrodynamic radius of P-2 at different concentrations.

Fig. 5. Plot of τ_f vs concentration.

Fig. 6. Time-dependent distribution of R_h for P-1 at 0.02 mg/mL.

Fig. 7. Time-dependent scattering intensity of the ADPs with different DA.

Fig. 8. Change of the R_h with DA.

Table 1 The thermodynamic quantities of the ADPs.

DA	38%	41%	51%	60%
$\triangle H^0$/kJ mol^{-1}	-290	-241	-234	-213
$\triangle G^0$/ kJ mol^{-1}	-36	-37	-37	-38
$T\triangle S^0$/kJ mol^{-1}	-254	-205	-197	-176

Table 2. The relaxation time of the ADPs at 6×10^{-11} mol/mL.

DA	38%	41%	51%	60%
τ_1/s	602.5	372.5	241.6	204.0
τ_2/s	6556.8	4687.5	4872.7	4088.7
τ_f/s	1805.3	1781.6	1777.5	1267.3